Supporting Information

Glass transitions in pressure-collapsed ice clathrates and implications for cold water

Ove Andersson[1] and Akira Inaba[2]

[1] *Department of Physics, Umeå University, 901 87 Umeå, Sweden*

[2]*Research Center for Structural Thermodynamics*, *Graduate School of Science, Osaka University*, *Toyonaka, Osaka 560-0043*, *Japan.*

Experimental Method

Heat capacity per unit volume c (the product of density and specific heat per unit mass) and thermal conductivity κ were measured *in situ* by the transient hot-wire method. [1,2] Briefly, a 0.1- or 0.3-mm Ni wire was heated by a square pulse of 1.4 s (or 14 s to test the effect of the changed probe time) duration, which increased the wire temperature by ~3.5 K. The increase occurs in a time-dependent manner, which is determined by c and κ of the sample. The increase was measured with time as a change in the resistance between two electrical potential taps on the hot wire, which was placed in a ring of constant radius within a Teflon® sample cell. The heat transfer equations for the wire and the surrounding solid are given by:

$$\frac{\partial^2 T}{\partial r^2}+\frac{1}{r}\frac{\partial T}{\partial r}-\frac{1}{a_w}\frac{\partial T}{\partial t}=-\frac{q}{\kappa_w \pi r_w^2} \qquad \text{(S1)}$$

$$\frac{\partial^2 T}{\partial r^2}+\frac{1}{r}\frac{\partial T}{\partial r}-\frac{1}{a}\frac{\partial T}{\partial t}=0$$

where t represents the time, T represents the temperature, r represents the radial coordinate, q represents the power per unit length, κ_w represents the thermal conductivity of the wire, and a and a_w represent the thermal diffusivity of the sample and wire, respectively. The exact solution of the temperature increase ΔT of an infinitely long and infinitely conducting wire immersed in an infinitely large sample is [3]

$$\Delta T=\frac{2q\alpha^2}{\pi^3\kappa}\int_0^\infty \frac{1-\exp(-\beta u^2)}{u^3\{(uJ_0(u)-\alpha J_1(u))^2+(uY_0(u)-\alpha Y_1(u))^2\}}du\,, \qquad \text{(S2)}$$

where $\alpha = 2c/c_w$, $\beta = \kappa t/(c\, r_w^2)$, r_w represents the radius of the wire, c_w represents the heat capacity per unit volume of the hot wire, J_0 an J_1 represent Bessel functions of the first kind of the zero and first orders, and Y_0 and Y_1 represent Bessel functions of the second kind of the zero and first orders.

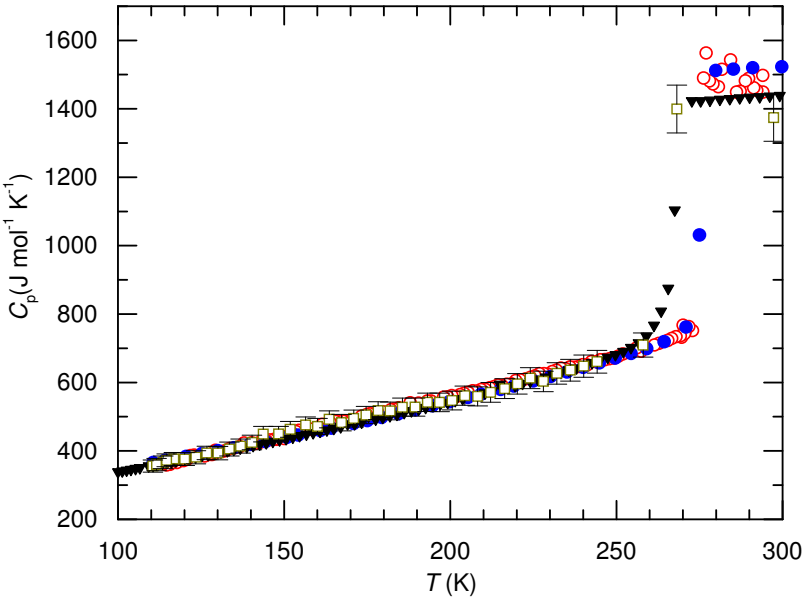

Figure S1. Molar heat capacity plotted against temperature. Results for: (○) THF·16.65 H_2O and (□) DXL·16.4 H_2O calculated from c data at ~0.05 GPa and density values at 1 atm (see text). Literature results of adiabatic heat capacity measurements at atmospheric pressure are shown for comparison: (●) THF·16.64 H_2O [6] and (▼) DXL·16.95 H_2O (lightly KOH doped) [7]. The results agree to within 3% at 130 K. The error bars correspond to a ±5% inaccuracy. The larger scatter in the liquid solutions at room temperature is due to convection.

A fit of eq S2 to the measured temperature increase of the hot wire yielded both c and κ, with uncertainties of approximately ±5% and ±2%, respectively. To demonstrate that the c (we use c_p for J kg^{-1} K^{-1} and C_p for J mol^{-1} K^{-1}) measured in our experiments yields C_p values almost similar to those measured by adiabatic calorimetry, we calculated C_p from the c data of the CHs and literature data for density. For THF·16.65 H_2O and DXL·16.34 H_2O, we calculated a density ρ of 0.99 and 1.00 g cm^{-3} g cm^{-3}, respectively, at 200 K using a cell dimension of 17.2 Å [4,5] and used previously reported thermal expansion data in the temperature range 100–300 K.[5] The plots of the calculated C_p data for THF·16.65 H_2O and DXL·16.34 H_2O measured during cooling at

~0.05 GPa are shown in Figure S1, where the known C_p of THF·16.64 H_2O [6] and DXL·16.95 H_2O [7] (doped with 1.8×10^{-4} mole KOH per mole H_2O) at 0.1 MPa is also plotted for comparison. The data agree to within 5% or better.

Hot-wire results near a glass transition.

On heating through a glass transition, the nonequilibrium state of the glass kinetically unfreezes and the resulting gain in configurational c appears as a sigmoidal-shaped increase in the plot of c against T. As is well known, the glass transition temperature is a function of the time scale used to analyze the heat exchange response with the sample. In the hot-wire analysis of the response to a normal 1.4-s or a prolonged 14-s heating pulse while the sample is simultaneously heated or slowly cooled by the surroundings at a rate less than 0.5 K min^{-1}, the measured kinetic unfreezing occurs within ~1 s (more exactly 0.2 ± 0.1 s at the onset of the c rise-see below) or ~10 s (transient heating rate of 3.5 K in 1.4 s or 14 s, which corresponds to 150 or 15 K min^{-1}). Thus, the slow heating or cooling rate caused by the surroundings does not affect the position of the sigmoidal-shaped increase in the temperature plane. These time scales are shorter than those of adiabatic calorimetry, where a transient pulse also heats the sample, but a waiting time of several minutes is required to reach equilibrium. Our technique also differs from differential scanning calorimetry (DSC) where the temperature of the sigmoidal-shaped heat capacity C_p increase is determined by the heating and cooling rates.

The heat capacity c data at the glass transition can be studied using a model for the time or frequency dependence [8] of the heat capacity in the glass transition range, as done previously for HDA,[9] and the results are reproduced here for convenience. The heat capacity per unit volume varies with time according to

$$c(t) = c_\infty + (c_0 - c_\infty)\, e^{-(t/\tau)^\beta}, \qquad \text{(S3)}$$

where c_0 and c_∞ represent the short and long time values associated with the glass and liquid states, respectively, τ represents the calorimetric relaxation time, and β represents an exponent between 0 and 1. That is, the total increase in c due to the glass transition is given by $c_\infty - c_0$. By inserting eq S3 in eq S1, the temperature increase in the wire probe can be calculated for a given relaxation time. A subsequent fit of eq S2 yields c, and the fraction of $c_\infty - c_0$, which is measured for a given relaxation time. The values of c_0 and c_∞ were chosen on the basis of experimental

values for HDA but their magnitudes are not critical. A very short relaxation time gives the liquid $c = c_\infty$, whereas a long relaxation time gives the glassy $c = c_0$. The shape of the increase depends on β, and $\beta = 0.5$ agreed well with the experimental data, as shown in Figure S2. The values of τ for the measured heat capacity increase $\triangle C_p$ versus temperature were calculated from the dielectric relaxation time versus temperature data.[10] The calculated c (or C_p) and the measured increase occur at slightly different τ, as shown in Figure S2. The shift in log (τ) of approximately 0.4 corresponds to a temperature difference of ~3.5 K, which indicates that there is only a slight difference between the dielectric and calorimetric relaxation times of HDA. The results for the calculated C_p increase in Figure S2 have been vertically scaled to best coincide with the experimental values. The dashed lines provide an error estimate of 10% in the C_p increase, which also includes the uncertainty in the baseline used to subtract the vibrational component of the experimental heat capacity. (The scaling procedure assumes that the temperature dependence of the dielectric and calorimetric relaxation times is roughly the same in the transition range.) The results indicate that ~90% of the total increase ($c_\infty - c_0$) has occurred when HDA crystallization intervenes at 153 ± 1 K and a C_p increase of 3.4 ± 0.2 J mol^{-1} K^{-1}.[9] In other words, if HDA crystallization can be prevented, these calculations indicate that the contribution from the kinetic unfreezing of the molecular motions at T_g would further increase C_p and give a total heat capacity increase of 3.7 ± 0.4 J mol^{-1} K^{-1} in the glass transition range.

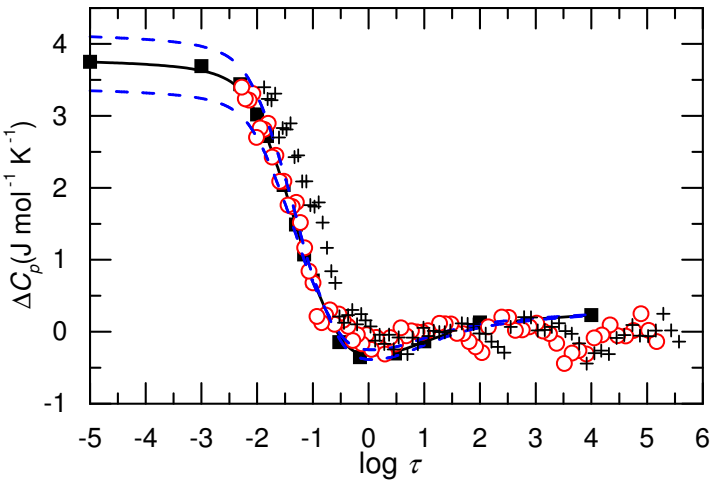

Figure S2. Heat capacity change as a function of the logarithm of the relaxation time (in s): (+) results for HDA plotted against the dielectric relaxation time and (○) the same data but shifted $\triangle \log \tau = -0.4$ to

coincide with the calculated values (■) (see text). The dashed lines provide an error estimate. The calculations indicate that the increase in the heat capacity occurs at a calorimetric relaxation time of 0.2 ± 0.1 s.

In this study, we typically used a heating pulse of 1.4 s, which is known to give low scatter. However, to test the influence of probe time, we also changed the electronics and software so that the measurements could be performed using a 14-s long heating pulse. This increased the scatter in the data, e.g., owing to effects caused by the reflection of the heat wave against the sample cell wall and changes in the temperature drift during the measurements, which is assumed to be constant. Data analysis of the 14-s pulse in various time ranges showed that the range between 1.5 s and 11 s gave acceptable scatter and was subsequently used for the complimentary long time-scale measurements.

Hot-wire results at crystallization.

When a sample crystallizes on heating, the temperature of the sample increases, and in the DSC technique, the resulting heat loss appears as an anomalous decrease in c with increasing T. The temperature of the sample also increases in our technique, but in this case, crystallization appears as an anomalous *increase* in c. This stems from the manner of crystal growth that generally occurs at random sites in the sample, but since the temperature increase and decay begins at the hot-wire probe in our technique, the wire acts not only as a nucleation site but also as a preferred growth site. The heat loss to the surroundings, without compensation (unlike DSC), adds to the temperature increase of the wire probe. Finite element analysis by using eq S1 and subsequent fitting of eq S2 showed that c artificially increases when an ice layer (or a layer with higher κ than that of the bulk) forms on the probe.[9]

Estimation of density for a collapsed CH at 1 GPa.

The density of THF-CH and DXL-CH at 130 K and 1 bar is approximately 1.00 g cm^{-3}, which is calculated from the cell constant of approximately 17.15 Å. [4,5] To approximately calculate the density at 1 GPa, we use Whalley's estimate that the compressibility of a CH is 1.162 times that of ice Ih.[11] The density of ice Ih increases ~10% on pressurization from 1 bar to 1 GPa at 125 K [12] by a short extrapolation from the transition pressure of 0.85 GPa, which yields an ~12% density increase for the CH. Accounting for the 30% density increase at the collapse and

subsequent slight densification on heating, which is observed for ice Ih,[13, 14] the density of the collapsed state would be approximately 1.5 g cm^{-3} at 1 GPa with an uncertainty of approximately 5%.

Table S1: Glass transition properties.

	T_g[a] (K)	ΔC_p J H_2O-$mol^{-1}K^{-1}$	$\triangle T$ (K)	$\tau_d\,(T_g)$[d] (s)
HDA	139.5 ± 1	3.7 ± 0.4[b]	-[c]	0.4 ± 0.05
Collapsed THF-CH	138.3 ± 1	3.7 ± 0.4	17 ± 1	0.35 ± 0.05
Collapsed DXL-CH	138.8 ± 1	3.9 ± 0.4	17 ± 1	-

[a]Results using a heating pulse of 1.4 s, which corresponds to a calorimetric relaxation time of approximately 0.2 ± 0.1 s at the onset of the heat capacity increase, as estimated from Figure S2.

[b]Estimated from calculations.[9]

[c]Interrupted by crystallization at 153 ± 1 K

[d]The (exact) dielectric relaxation times τ_d extracted from plots of log τ_d versus T^{-1}. [10, 15,16]

(1) Håkansson, B.; Andersson, P.; Bäckström, G. Improved hot-wire procedure for thermophysical measurements under pressure. *Rev. Sci. Instrum.* **1988**, *59*, 2269-2275.

(2) Andersson, O.; Inaba, A. Thermal conductivity of crystalline and amorphous ices and its implications on amorphization and glassy water. *Phys. Chem. Chem. Phys.* **2005**, *7*, 1441-1449.

(3) Carslaw, H. S.; Jaeger, J. C. *Conduction of heat in solids*; 2nd ed. Clarendon: Oxford, 1959, pp 341.

(4) Gough, S. R.; Davidson, D. W. Composition of tetrahydrofuran hydrate and the effect of pressure on the decomposition. *Can. J. Chem.* **1971**, *49*, 2691-2699.

(5) Hester, K. C.; Huo, Z.; Ballard, A. L.; Koh, C. A.; Miller K T.; Sloan, E. D. Thermal Expansivity for sI and sII Clathrate Hydrates. *J. Phys. Chem. B* **2007**, *111*, 8830-8835.

(6) Yamamuro, O.; Oguni, M.; Matsuo, T.; Suga, H. Calorimetric study of pure and KOH-doped tetrahydrofuran clathrate hydrate. *J. Phys. Chem. Solids* **1988**, *49*, 425-434.

(7) Yonekura, T.; Yamamuro, O.; Matsuo, T.; Suga, H. Calorimetric and DTA studies of 1,3-dioxolane hydrate and (1,3-dioxolane)$_{1-x}$ (tetrahydrofuran)$_x$ mixed hydrates. *Thermochim. Acta* **1995**, *266*, 65-77.

(8) Birge, N. O.; Nagel, S. R. Specific-Heat Spectroscopy of the Glass Transition. *Phys. Rev. Lett.* **1985**, *54*, 2674-2677.

(9) Andersson, O. Glass–liquid transition of water at high pressure. *Proc. Natl. Acad. Sci. USA* **2011**, *108*, 11013-11016.

(10) Andersson, O.; Inaba, A. Dielectric properties of high-density amorphous ice under pressure. *Phys. Rev. B* **2006**, *74*, 184201.

(11) Whalley, E. Speed of Longitudinal Sound in Clathrate Hydrates. *J. Geophys. Res.* **1980**, *85*, 2539-2542.

(12) Gromnitskaya, E. L.; Stal'gorova, O. V.; Brazhkin, V. V.; Lyapin, A. G. Ultrasonic study of the nonequilibrium pressure-temperature diagram of H_2O ice. *Phys. Rev. B* **2001***, 64*, 094205.

(13) Mishima, O. Reversible first-order transition between two H_2O amorphs at ~0.2 GPa and ~135 K. *J. Chem. Phys.* **1994**, *100*, 5910-5912.

(14) Loerting, T.; Salzmann, C.; Kohl, I.; Mayer, E.; Hallbrucker, A. A second distinct structural "state" of high-density amorphous ice at 77 K and 1 bar. *Phys. Chem. Chem. Phys.* **2001**, *3*, 5355-5357.

(15) Andersson, O. Relaxation time of water's high-density amorphous ice phase. *Phys. Rev. Lett*. **2005**, *95*, 205503.

(16) Andersson, O.; Johari, G. P. Nature of the pressure-induced collapse of an ice clathrate by dielectric spectroscopy. *J. Chem. Phys.* **2008**, *129*, 234505.